An Application of the Observer/Kalman Filter Identification (OKID) Technique to Hubble Flight Data

Jer-Nan Juang, Lucas G. Horta, W. Keith Belvin
NASA Langley Research Center
Hampton, VA 23665

John Sharkey
Marshall Space Flight Center
Huntsville, AL 35812

Frank H. Bauer
Goddard Space Flight Center
Greenbelt, MD 20771

The objective of the current research is to identify vibration parameters, including frequencies, damping ratio and uncertainty characteristics, of the Hubble Space Telescope from flight data using an advanced system identification technique. The Observer/Kalman Filter Identification (OKID) technique is used to identify the vibration parameters. The OKID was recently developed by the researchers in the Spacecraft Dynamics Branch at NASA Langley Research Center.

OUTLINE

- Description of the Observer/Kalman Filter Identification (OKID)
- Brief Description of the Hubble Flight Data
- Identification Results

System identification is to develop or improve a mathematical model of a physical system using experimental data. The development of a model can be performed by processing the data in the frequency domain or time domain. The conventional identification methods in the structures field use the frequency-based transfer function matrix or the time-based free-decay responses for model representation. The knowledge of either the transfer function matrix or the free decay responses makes it possible to construct a data matrix as the basis for the identification of modal parameters including frequencies, damping ratio and mode shapes at the sensor points. The Eigensystem Realization Algorithm (ERA) or Eigensystem Realization Algorithm using Data Correlation (ERA/DC) developed in the Spacecraft Dynamics Branch was based on the data matrix from pulse response to compute a state space discrete-time model or the modal parameters. Recently, a time-based technique was developed for computation of pulse response samples directly from input and output data without using the frequency-based transfer function. Because it is a time domain technique, data periodicity is not needed as in most frequency-based procedures. The pulse responses thus computed include information of not only the system but also the characteristics of the system uncertainties, which lead to separate identification of the system model and its corresponding observer using ERA. This newly developed technique is now called the Observer/Kalman Filter Identification (OKID).

OBSERVER/KALMAN FILTER IDENTIFICATION (OKID)

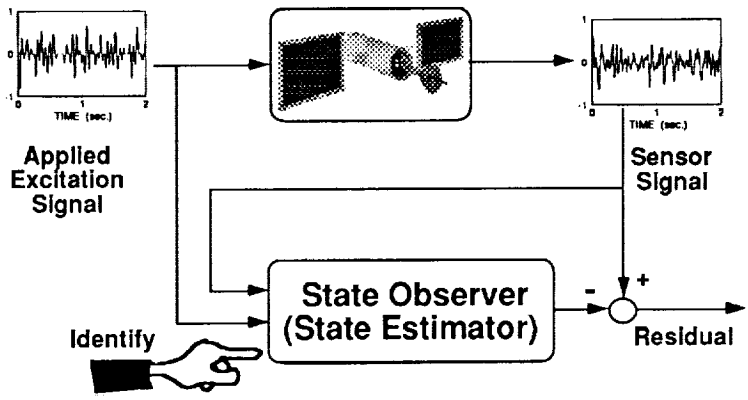

- Identify a state space model and its corresponding observer/Kalman filter directly from input and output data for modal parameter identification or controller designs.

There are basically two ways to stochastically characterize system uncertainties including plant and measurement noises. One way is to describe the input and output uncertainties directly in terms of their covariances. Another way is to specify the Kalman filter equation with its steady state Kalman gain which is a function of the input and output uncertainty covariances. In the OKID, an observer is identified to characterize the input and output uncertainties. If the data length is sufficiently long, and the number of identified observer Markov parameters (pulse response time histories) is sufficiently large, then the identified observer of the system order approaches the Kalman filter.

CHARACTERIZATION OF UNCERTAINTIES

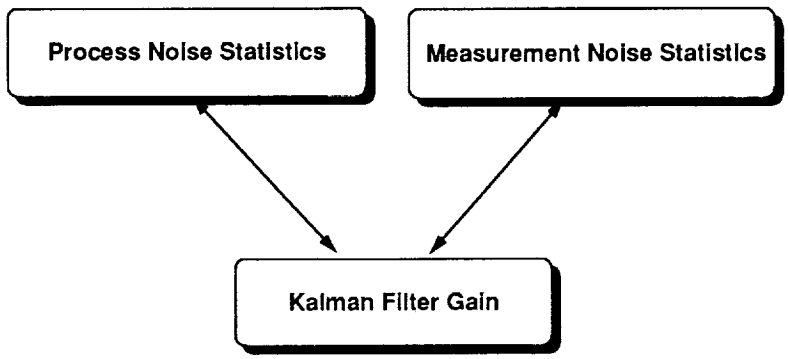

The OKID has two ways of processing the input and output data for system identification. One is the forward-in-time and the other is the backward-in-time. The forward-in-time means that the current output measurement can be fully estimated by the previous inputs and outputs, and is commonly used for the system identification. If one reverses time in the model to be identified, then what were damped true system modes become undamped true system modes, growing as the reversed time increases. Physically, it implies that the current output measurement can be fully estimated by the future inputs and outputs. On the other hand, the noise modes in the forward and backward identification still maintain the property that they are stable. This is intuitively reasonable. If the data set is sufficiently long, an unstable noise mode would predict noise contributions to the pulse response data that grow unbounded as the time step in the data set increases. This is inconsistent with the expected contribution of noise in data. Therefore, the backward identification has the advantage of shifting from positive damping to negative damping of the true system modes to distinguish these modes from noise modes. Real experiences have shown that the backward identification may fail to indicate certain system modes in experimental data, perhaps due to the unmatched uncertainty levels in forward and backward identification.

OBSERVER/KALMAN FILTER IDENTIFICATION (OKID)

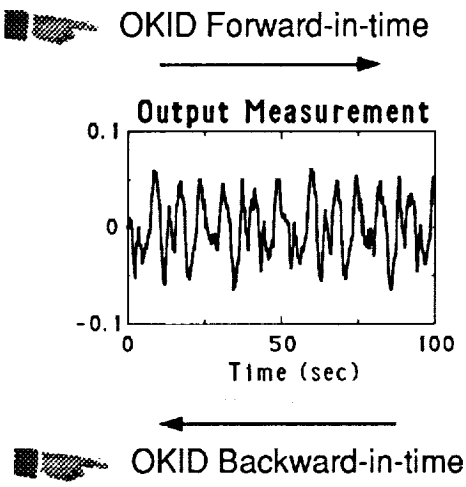

Given a set of experimental input and output data, the identification algorithm proceeds as follows.

Step 1: Choose a value of *p* which determines the number of observer Markov parameters to be identified from the given set of input and output data. The product of the number p and the number of sensors is required to be larger than the effective order of the system for identification of a state space model.

Step 2: Recover the combined system and observer gain pulse response samples from the identified observer Markov parameters.

Step 3: Realize a state space model of the system and the corresponding Kalman filter gain from the recovered pulse response samples using ERA or ERA/DC.

OKID ROAD MAP

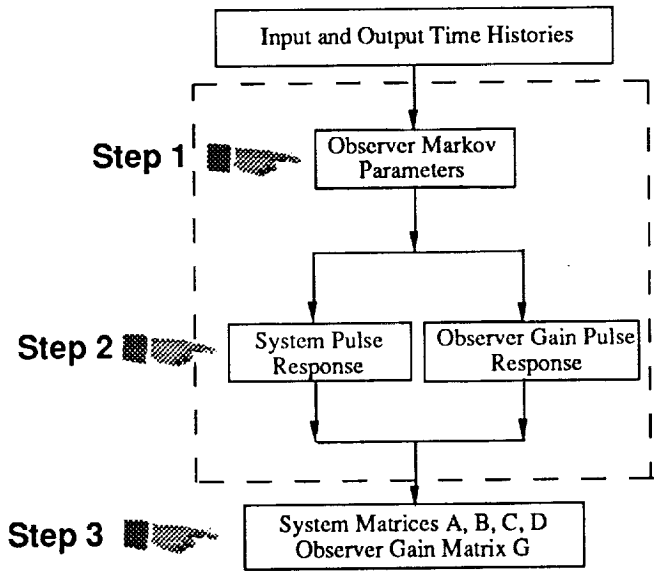

There are six gyros located on the Optical Telescope Assembly (OTA) and four torque wheels located on the Spacecraft Subsystem Module (SSM). The OTA is fixed inside the SSM. The gyros are used mainly to measure the motion of the primary mirror. Data from four out of the six gyros are recorded at a time. The measurement resolution is 0.005 arcsec/sec which implies that the gyro data are not adequate because the requirement is 0.007 arcsec pointing. The angular rates, which are measured along the four gyro directions, are combined and transformed using least-squares to recover the three rates in vehicle coordinates. Least-squares is used to smooth the poor resolution of the data. The input commands are given in terms of angular acceleration in the three rotational vehicle coordinates and then projected on the four torque wheel axes to excite the telescope mirror and the spacecraft. The data are sampled at 40 Hz. Pulses combined with sine-sweeping in the middle of an excitation period (50.975 sec) were used as input commands to the torque wheels. The excitation period was repeated six times for a total of approximately 12,000 samples taken for each experiment. The experiment was repeated three times for the other two vehicle coordinates. As a result, there were three inputs and four outputs for a total of three sets of 12,000 input samples and twelve sets of 12,000 output samples to be used for identification of vibration parameters.

HUBBLE SPACE TELESCOPE

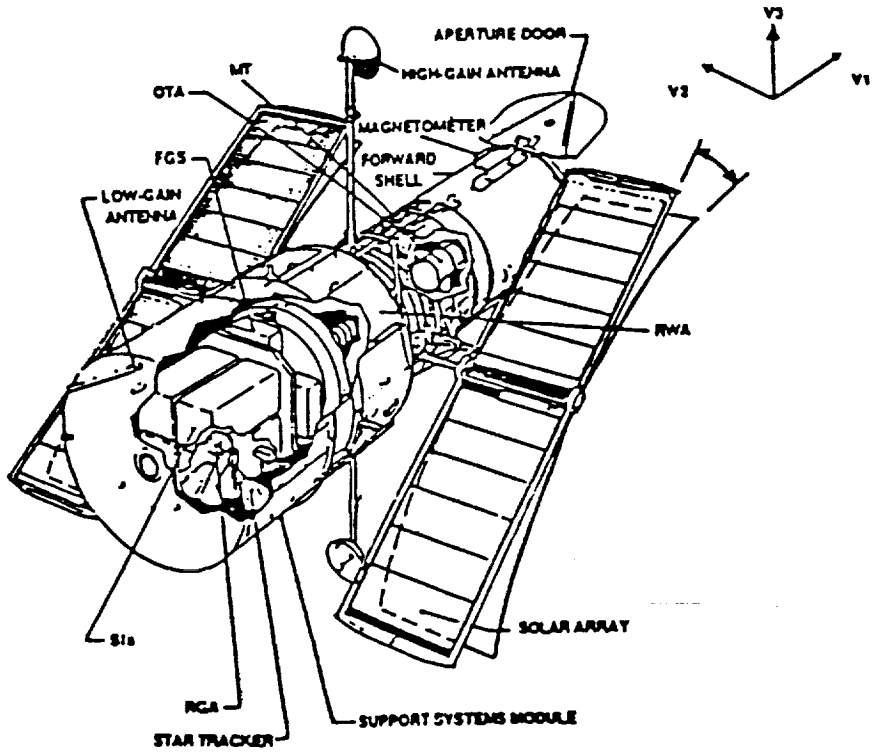

The usual practice of modal parameter identification uses the Fast Fourier Transforms (FFT) of the inputs and measured outputs to compute the sampled pulse response histories. A somewhat rich input is required to prevent numerical ill-conditioning in the computation. Another approach is to solve directly in the time domain for the pulse response histories from the input and output data. The drawbacks of this method include the need to invert an input matrix which necessarily becomes particularly large for lightly damped systems. Rather than identifying the pulse response histories directly which may exhibit very slow decay, the OKID uses an asymptotically stable observer to form a stable state space discrete model for the system to be identified. The primary purpose of introducing an observer is to compress the data and improve system identification results in practice. As shown in the figure, the input and output time histories are several order longer than the observer pulse response histories (observer Markov parameters). The modal parameters which are excitable by the inputs and measurable by the output sensors are embedded in the identified observer Markov parameters.

COMPUTATION OF OBSERVER MARKOV PARAMETERS (OKID - Step 1)

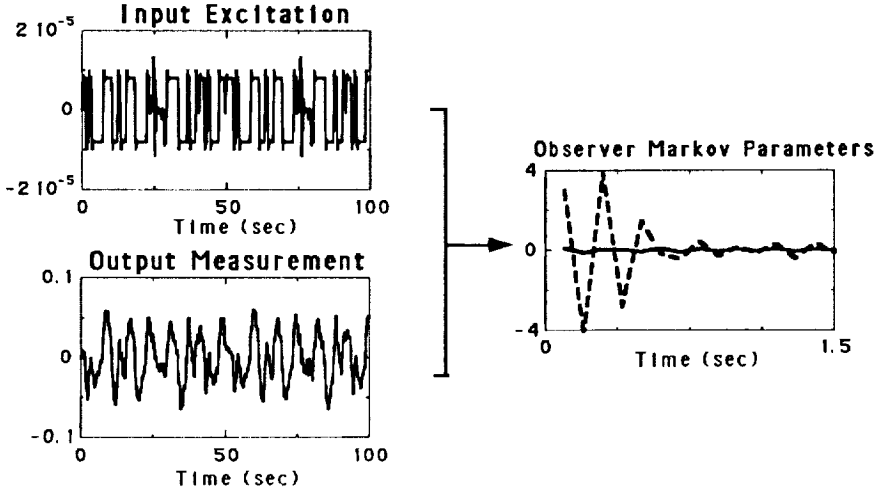

From the identified observer Markov parameters, the system pulse responses and the observer gain pulse responses can be easily computed using the formulations derived for the OKID. Although the number of identified observer Markov parameters is finite and generally very small, the number of system pulse response samples can be as large as desired. Note that the maximum number of independent system pulse response samples is equal to the number of identified observer Markov parameters. To solve for more system pulse response samples than the number of identified observer Markov parameters, simply set the extra observer Markov parameters to zero.

COMPUTATION OF PULSE RESPONSES (OKID - Step 2)

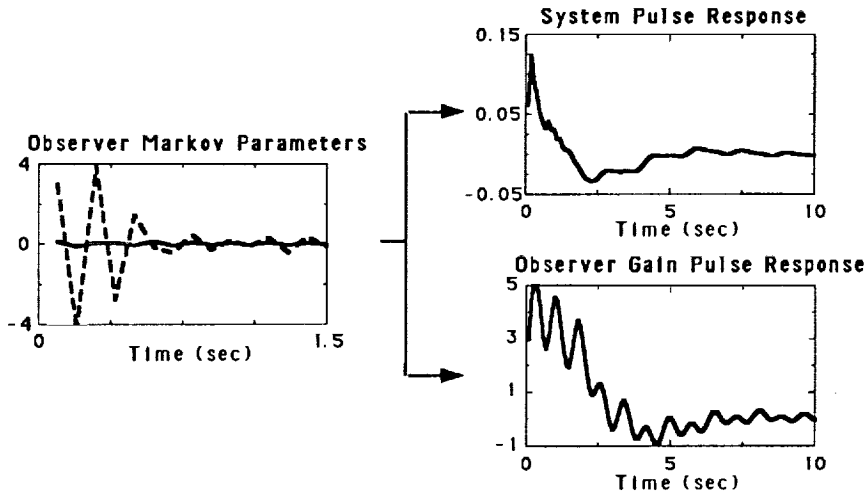

Knowledge of the actual system response samples allows one to use the ERA or ERA/DC to obtain a state-space realization of the system of interest. Modal parameters including natural frequencies, damping ratios, and mode shapes can then be found. In addition, the OKID can go further to identify an observer gain using the identified observer gain pulse response samples. The identified observer gain is related to the steady state Kalman filter gain which may be used to characterize the system uncertainties and measurement noises.

COMPUTATION OF SYSTEM MODEL BY ERA (OKID - Step 3)

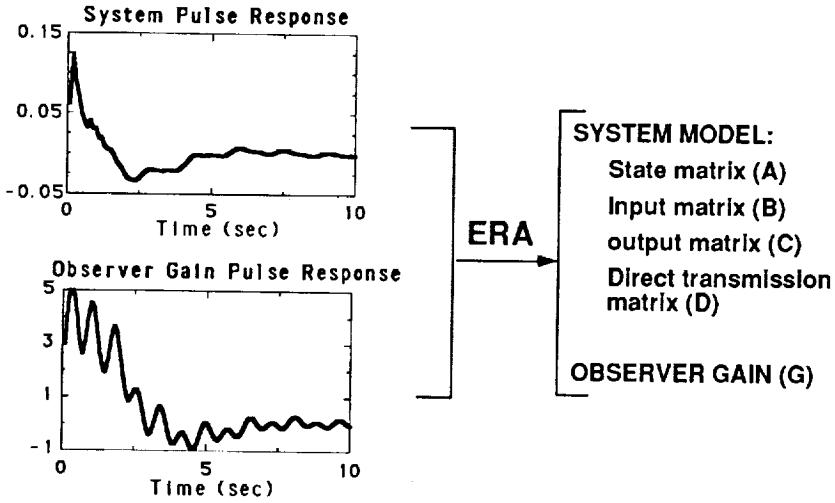

A linear model and observer were identified for the Hubble Space Telescope. The system order was chosen to be 30 for realization of the system matrices, using the identified observer Markov parameters. Seven dominant modes were identified. The Mode SV in the table describes the singular value contribution of each individual mode to the pulse responses. It has been normalized relative to the maximum singular value. The 0.65 Hz mode is believed to be an In-plane bending mode of the solar array; the 1.29 Hz mode is a coupled solar and membrane mode; and the 2.45 Hz mode is the first mode of the primary deployment mechanism with the solar array housing attached. The identified dampings are higher than expected because there is an attitude control for maneuvering during testing and mechanical friction of the solar array mechanism.

FORWARD AND BACKWARD IDENTIFICATION

Forward Identification			Backward Identification		
Freq. (Hz)	Damping (%)	Mode SV	Freq. (Hz)	Damping (%)	Mode SV
0.147	55.6	0.76	0.161	46.3	0.84
0.155	58.4	0.98	0.151	47.6	0.88
0.169	67.4	1.00	0.166	29.6	1.00
0.633 [1]	5.73	0.68			
1.273 [2]	4.06	0.37			
2.433 [3]	5.23	0.02			
2.822	6.33	0.01			

[1] In-plane bending mode of the solar panel

[2] Coupled solar and membrane mode

[3] First mode of the primary deployment mechanism with the solar array housing attached

The left figure shows the excitation input signal including pulse combined with a sine-sweeping signal in the middle of an excitation period (50.975 sec). The figures on the right-hand side show a 50-second overlap of the reconstruction from the identified forward and backward system models, and the test data for the first vehicle axis. There are some visible differences in the backward identification between test and reconstruction, but overall the map from the input to the output is reasonably well. The forward identification is somewhat better than the backward identification in damping estimation. The damping ratio estimated from the backward approach appears to be a little low. It is important that the system model be accurate because it is this part that is used as a model for control design.

COMPARISON OF REAL AND RECONSTRUCTED DATA (Vehicle Axis #1)

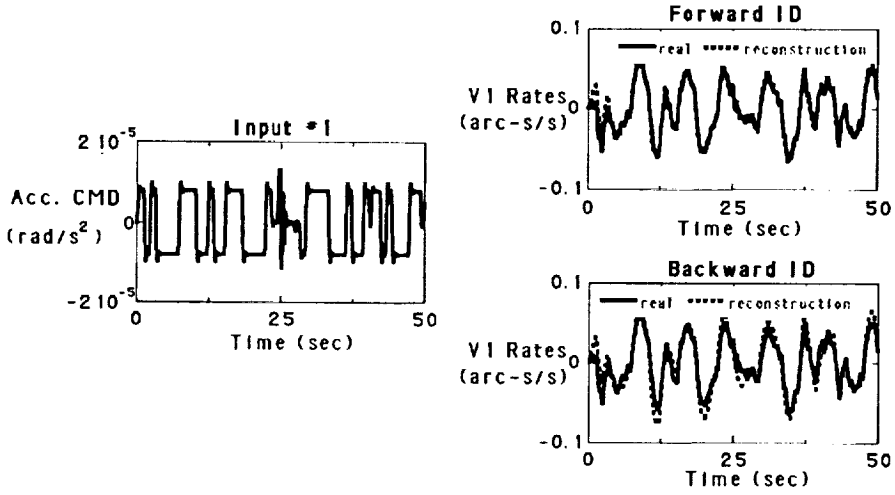

The left figure shows the excitation input signal including pulse combined with a sine-sweeping signal in the middle of an excitation period (50.975 sec). The excitation signal starting from approximately 60 seconds for the second vehicle axis is identical to that for the first vehicle axis. The figures on the right-hand side show a 50-second overlap of the reconstruction from the identified forward and backward system models, and the test data for the second vehicle axis. There are relatively more visible differences in the backward identification between test and reconstruction in comparison with the results shown in the last chart for the first vehicle axis. The forward identification is obviously better than the backward identification in this case.

COMPARISON OF REAL AND RECONSTRUCTED DATA (Vehicle Axis #2)

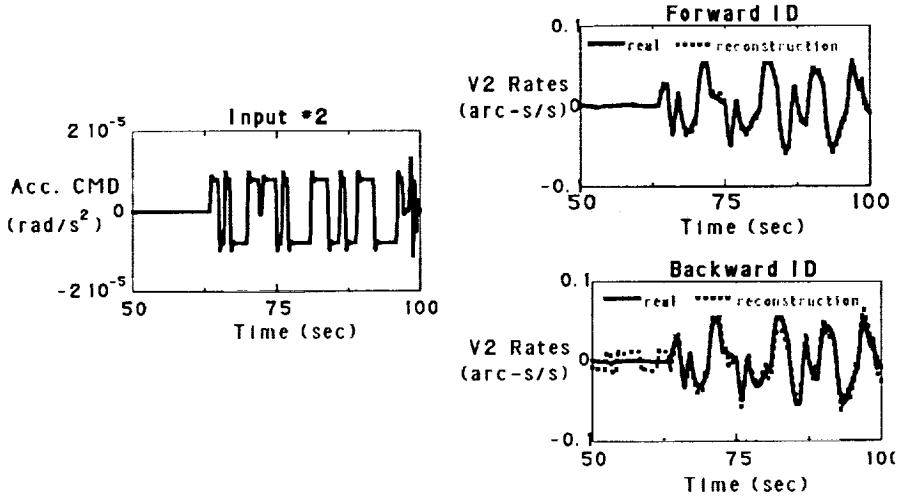

The left figure shows 50 seconds of an excitation input signal including pulse combined with a sine-sweeping signal in the middle of an excitation period (50.975 sec). The excitation signal starting from approximately 150 seconds for the third vehicle axis is identical to that for the first vehicle axis. The two figures on the right-hand side show a 50-second overlap of the reconstruction from the identified forward and backward system models, and the test data for the third vehicle axis. There are only very little visible differences between test and reconstruction, implying that the input/output map is excellent.

COMPARISON OF REAL AND RECONSTRUCTED DATA
(Vehicle Axis #3)

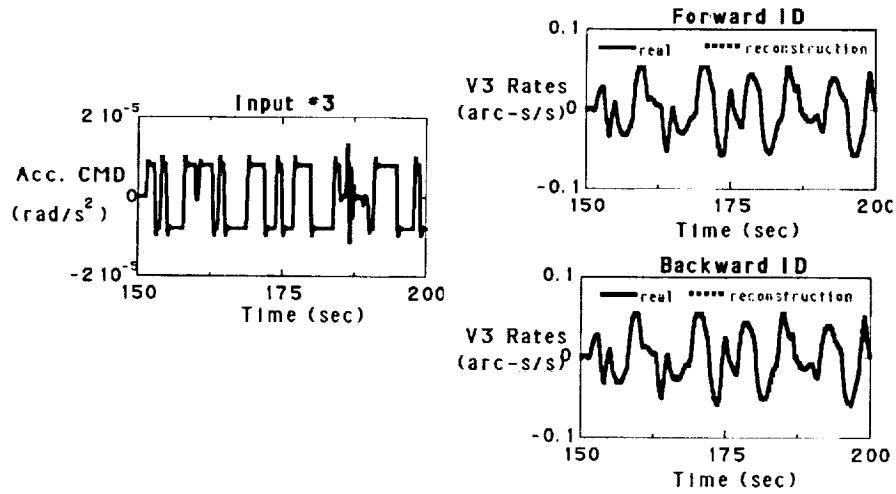

The left figure shows the excitation input signal including pulse combined with a sine-sweeping signal in the middle of an excitation period. The figures on the right-hand side show a 50-second overlap of the reconstruction from the identified forward system models, and the test data for the first vehicle axis. The figure in the right-hand upper corner shows the predicted output in comparison with the real output data. The figure in the right-hand lower corner shows the estimated output in comparison with the real output data. The predicted output is the output reconstructed from the identified model only whereas the estimated output is the output reconstructed from the identified observer. There are visible differences in the predicted and estimated outputs. Comparison of the observer output with the measured response shows extremely good agreement, indicating that the observer is correcting for the system uncertainties including nonlinearities. The covariance of the estimated output residuals is about three order less than the predicted output residuals. Similar results of the predicted and estimated outputs were obtained for the second and third vehicle axes, and thus are not shown in this presentation.

COMPARISON OF PREDICTED AND ESTIMATED OUTPUT (Vehicle Axis #1)

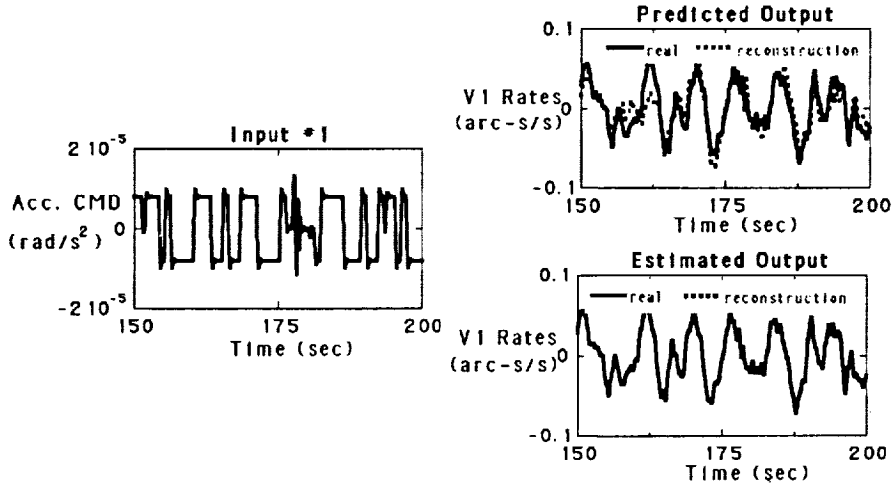

The identified system model obtained by this method incorporates information about unmodeled dynamics and measurement noises into a system observer model. A system observer identified from measured response data is available for direct use in observer-based control law designs. Also the identified observer can be used to characterize system uncertainties and measurement noises which often require considerable engineering insight and judgement.

CONCLUDING REMARKS

- The identified dampings are high due to an attitude control for maneuvering during testing and mechanical friction of the solar array mechanism.
- The response of the identified model has good correlation with the measured response.
- Comparison of the observer output with the measured response shows extremely good agreement, indicating that the observer is correcting for the system uncertainties.
- The identified observer model is available for direct use in observer-based control law designs.
- Further analysis of the existing Hubble flight data is undertaken to simultaneously identify the attitude controller and the open-loop system.

Bibliography:

[1] Juang, J.-N., and Pappa, R. S.," An Eigensystem Realization Algorithm for Modal Parameter Identification and Model Reduction," Journal of Guidance, Control, and Dynamics, Vol. 8, No. 5, Sept.-Oct. 1985, pp. 620-627.

[2] Juang, J.-N., Cooper, J. E., and Wright, J. R., "An Eigensystem Realization Algorithm Using Data Correlations (ERA/DC) for Modal Parameter Identification," Control-Theory and Advanced Technology, Vol. 4, No. 1, 1988, pp. 5-14.

[3] Chen, C. W., Huang, J.-K., Phan, M., and Juang, J.-N.,"Integrated System Identification and Modal State Estimation for Control of Large Flexible Space Structures," Journal of Guidance, Control and Dynamics, Vol. 15, No.1, Jan.-Feb. 1992, pp. 88-95.

[4] Phan, M., Juang, J.-N., and Longman, R. W., "Identification of Linear Multivariable Systems from a Single Set of Data by Identification of Observers with Assigned Real Eigenvalues," Proceedings of the AIAA 32nd Structures, Structural Dynamics & Materials Conference, Baltimore, MD., April 8-10, 1991.

[5] Phan, M., Horta, L. G., Juang, J.-N., and Longman, R. W., "Linear System Identification Via an Asymptotically Stable Observer," Proceedings of the AIAA Guidance, Navigation and Control Conference, New Orleans, Louisiana, Aug. 1991, NASA Technical Paper 3164, 1992.

[6] Juang, J.-N., Phan, M., Horta, L. G.,and Longman, L. G., "Identification of Observer and Kalman Filter Markov Parameters: Theory and Experiments," Proceedings of the AIAA Guidance, Navigation and Control Conference, New Orleans, Louisiana, Aug. 1991.

[7] Horta, L. G., Phan, M., Juang, J.-N., Longman, R. W., and Sulla, J., "Frequency Weighted System Identification and Linear Quadratic Controller Design," Proceedings of the AIAA Guidance, Navigation and Control Conference, New Orleans, Louisiana, Aug. 1991.

[8] Phan, M., Juang, J.-N., and Longman, R. W., "On Markov Parameters in System Identification," NASA Technical Memorandum TM 104156, Oct. 1991.

[9] Juang, J.-N. and Phan, M., "Identification of Backward Observer Markov Parameters: Theory and Experiments," NASA TP-3164, June 1992.

[10] Hollkamp, J.J. and Batill, S.M., "Automated Parameter Identification and Order Reduction for Discrete Series Models," AIAA Journal, Vol. 29, No. 1, 1991.

[11] Juang, J.-N., Horta, L. G., and Juang, J.-N., "System/Observer/Controller Identification Tool Box," NASA Technical Memorandum TM-107566, Dec. 1991.

SESSION II

Chairman: Jerome Pearson
Wright Laboratory
WPAFB, Ohio

Co-Chairman: James Fanson
Jet Propulsion Laboratory
Pasadena, California